

Mathematical Modeling For The Reactive Power Requirements of Asynchronous Generator

Dr. Bhagwan Shree Ram

Professor, School of Electronics and Electrical Engineering

Lovely Professional University

Phagwara, Punjab, India

Email: bhagwan.24828@lpu.co.in

Abhishek Kumar Sinha

Assistant Professor, School of Electronics and Electrical Engineering

Lovely Professional University, Phagwara, Punjab, India

Email: abhishek.20356@lpu.co.in

Abstract: In this research paper selecting the value of the series compensation capacitance C_{se} , of an Self Excited Induction Generator, one should consider the voltage drop across C_{se} as well as the amount of compensating reactive power obtainable. A large value of C_{se} results in a smaller voltage drop, but the reactive power $I_L^2 X_{se}$ is also small. On the other hand, a small value of C_{se} results in a larger voltage drop but provides more reactive power for voltage compensation. At least one of the terminal impedances Z_1 , Z_2 , Z_3 and must contain a capacitive element in order to furnish the reactive power necessary for initiating self-excitation. Since the SEIG supplies isolated loads, the frequency of the output voltage is variable even when the rotor speed is maintained constant. The detailed mathematical model applying the Steinmetz connection has been presented in this research paper.

Index Terms—Induction generators, pattern search method, self-excitation, series compensation, Steinmetz connection.

I. INTRODUCTION

Exploitation of renewable energy resources and the development of autonomous power systems has led to popular use of self-excited induction generators (SEIGs) [16, 9 and 6]. Since many autonomous power systems supply single-phase loads, single-phase induction generators need to be used [15]. Single-phase induction motors can be operated as SEIGs [17, 13 and 21], but in general they are limited to relatively small power

outputs. SEIG ratings by more than 7.5 HP, 3-phase induction machines are cheaper and easily available in the market. Al-Bahrani and Malik [1] analyzed the single-phasing mode of operation of a three-phase induction generator in which the excitation capacitance and the load were connected in parallel. Since only two phases of a star-connected generator were involved in the energy conversion process, the winding utilization was poor and the machine phases were severely unbalanced. More recently, Fukami *et al* developed a self-excited single-phase asynchronous generator using a 3-phase machine [18]. By including series compensation capacitances, the voltage regulation was improved. However, the generator winding configuration was also one that gave the single-phasing mode of operation. Phase unbalance was again a problem and only an output power of 1 kW was obtained from a machine rated at 2.2 kW.

Better utilization of renewable energy may be achieved by developing small-scale, autonomous power systems in favorable geographic locations. The system cost can be minimized by the use of cage-type, self-excited induction generators (SEIGs). Over the past two decades, there has been rigorous research on SEIGs, encompassing such aspects as steady-state and transient analysis [16], capacitance requirement [20], voltage compensation [7], frequency control [8], and parallel operation [5]. Most of the published work focused on three-phase SEIGs with balanced excitation capacitances and loads. When the power ratings of the generator and loads become smaller, however, it becomes increasingly difficult to ensure an even distribution of the loads among the phases, which means that in general the SEIG has to operate with a certain degree of phase imbalance.

Autonomous power systems often employ single-phase distribution schemes for reasons of low cost, ease of maintenance and simplicity in protection [15]. The inherent phase imbalance in the machine will result in poor generator performance such as over-current and over-voltage, poor efficiency, excessive temperature rise and machine vibration. These undesirable effects can be alleviated to a large extent by the use of the Steinmetz connection [19] in which the excitation capacitance and load are connected across different phases. For isolated operation, however, perfect phase balance cannot be achieved for a pure resistive load [22] or a series R–L load [2]. The objectives of the paper are to develop a general method for analyzing the performance of a 3-phase SEIG under unbalanced operating conditions and to investigate a novel phase-balancing scheme for the SEIG when supplying single-phase loads.

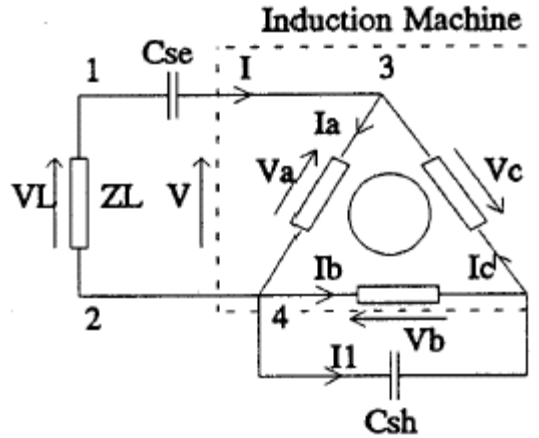


Fig. 1. Circuit connection of 1-phase SRSEIG .

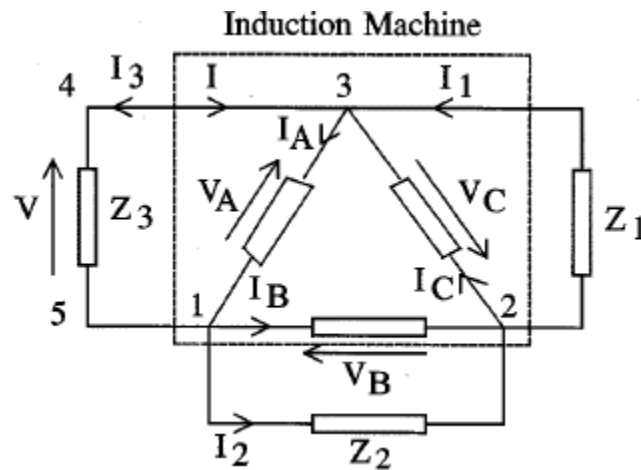


Fig. 2. Asymmetrically connected terminal impedances 3-phase SEIG.

II. CIRCUIT CONNECTION OF SRSEIG

Figure 1 shows the circuit connection of the single-phase SRSEIG based on the Steinmetz connection. The single-phase load connected across the phase A as the reference phase, while the excitation capacitance C_{sh} is connected across phase B (the lagging phase). Besides providing the reactive power for initiating and sustaining self-excitation, C_{sh} also acts as a phase balancer. The compensation capacitance C_{se} is in series with the load and provides additional reactive power when the load current increases. To facilitate analysis, all the voltages and the equivalent circuit parameters have been referred to the base (rated) frequency f_{base} by introducing the following parameters:

- 1) Per-unit frequency a , defined by:

$$a = (\text{Actual frequency})/(\text{Base frequency})$$
- 2) Per-unit speed b , defined by:

$$b = \text{Ratio of the Actual rotor speed to the Synchronous speed corresponding to the base frequency.}$$

III. STEADY-STATE ANALYSIS

Referring to Fig. 1 and adopting the motor convention for the direction of currents, the following “inspection” equations can be written [10]:

$$V = V_a \tag{1}$$

$$V_a + V_b + V_c = 0 \tag{2}$$

$$I_l = V_b Y_{ab} = I_c - I_b \tag{3}$$

$$I = I_a - I_c \tag{4}$$

In (3), Y_{sh} is the complex admittance of the excitation capacitance given by:

$$Y_{sh} = 1 / Z_{sh} = j2\pi f_{base} C_{sh} a^2 \tag{5}$$

Solving the above equations using symmetrical components analysis, the positive- and negative-sequence voltages are determined as follows:

$$V_p = \sqrt{3} V [Y_n + Y_{sh} (e^{j\pi/6} / \sqrt{3})] / [Y_{sh} + Y_p + Y_n] \tag{6}$$

$$V_n = \sqrt{3} V [Y_p + Y_{sh} (e^{-j\pi/6} / \sqrt{3})] / [Y_{sh} + Y_p + Y_n] \tag{7}$$

The input impedance of the induction generator across terminals 3 and 4 can be expressed as:

$$Z_{in} = (Z_p Z_n + Z_p Z_{sh} + Z_n Z_{sh}) / (3 Z_{sh} + Z_p + Z_n) \tag{8}$$

Details of the +ve sequence impedance Z_p and the -ve sequence impedance Z_n are given in Appendix I. For successful voltage build-up, the sum of impedances in loop 1243 must be equal to zero, i.e

$$Z_{in} + Z_L + Z_{sc} = 0 \tag{9}$$

Where $Z_L = R_L / a + j X_L$ \tag{10}

and, $Z_{sc} = 1 / (j2\pi f_{base} .C_{sc} a^2)$ \tag{11}

By Newton - Raphson method we can find out ‘a’ and X_m can be established.

For a given operating condition, (9) may be solved to give the per-unit frequency and the magnetizing reactance . The generator performance can then be calculated using (1) – (7), the symmetrical components equations, and the magnetization curve of the induction machine.

IV. SOLUTION PROCEDURE

An examination of (8) shows that the input impedance Z_{in} is a complicated function of the variables a and X_m , due to the multiplication and division involving the complex impedances Z_p , Z_n and Z_{sh} . It is thus very difficult to solve (9) using conventional techniques, i.e., rewriting (9) as two nonlinear equations in and solving them simultaneously using the Newton Raphson method [16]. In this paper, a method that requires much less computational effort is used for solving (9). For this purpose, the following impedance function is first established:

$$Z(a, X_m) = [(R_{in} + RL /a)^2 + (X_{in} + X_L + X_{se})^2]^{1/2} \tag{12}$$

Equation (9) is satisfied when the function in (12) is equal to zero (i.e., a minimum). The solution of (9) is thus reduced to a function minimization problem. To minimize the function Z , the pattern search method developed by Hooke and Jeeves [4] has been applied. The method relies only on function evaluations, and employs two strategies, namely exploratory moves and pattern moves, in order to arrive at the optimum point. For normal operation of an SEIG, a must be lower than that of the PU speed denoted by b and X_m must be less than the unsaturated value X_{mu} , hence b and X_{mu} can in general be chosen as initial estimates of a and X_m respectively for starting the search procedure. But when the load impedance is small, it may be necessary to use smaller initial values, say $0.95b$, in order to reduce the number of function evaluations. To facilitate discussion, a parameter called the compensation factor is defined as follows:

$$K = (C_{sh} / X_{se}) = (X_{sh} / C_{se}) \tag{13}$$

where X_{se} and X_{sh} are the reactance of the series compensation capacitance and shunt excitation capacitance, respectively.

V. PERFORMANCE ANALYSIS

Figure 2 shows the circuit connection of a delta-connected induction generator with asymmetrically connected terminal impedances. To simplify the analysis, all the circuit parameters have been referred to the base frequency referred as f_{base} by applying the PU frequency and the per-unit speed b [14]. Thus, the per-unit slip of the SEIG is $(a-b) / a$ and each voltage shown in Fig. 2 has to be multiplied by b in order to give the actual value. The circuit model shown in Fig. 2 can be used to study practically all modes of unbalanced operation of the SEIG in which zero-sequence quantities are absent. By assigning appropriate values to the terminal impedances, a specific unbalanced operating condition can be simulated.

A star-connected SEIG can also be analyzed by first transforming the generator to an equivalent delta-connected machine whose per-phase impedance is three-times the actual star-connected value. In the case of star-connected load impedances and excitation capacitances with isolated neutral points, star–delta transformation can likewise be applied to yield the equivalent delta-connected impedance values. After these

transformation procedures, the circuit will be reduced to the generic form as shown in Fig.2. For loads to be supplied by a four-wire system, a delta–star connected transformer can be placed between the generator and the loads so that zero-sequence currents are excluded from the SEIG. With appropriate impedance transformations, the system is again reduced to that as shown in Fig. 2.

In the present analysis, the method of symmetrical components is employed in order to account for the unbalanced circuit conditions. Since there is no active voltage source, the SEIG may be regarded as a passive circuit when viewed across any two stator terminals. For convenience, -phase is chosen as the reference and the input impedance of the SEIG across terminals 1 and 3 in Fig. 2 will be considered. Adopting the motor convention for the phase currents, the following “inspection equations” [11] may be written:

$$V = V_A \tag{14}$$

Zero sequence voltages and current are absent.

$$V_A + V_B + V_C = 0 \tag{15}$$

For C-phase

$$I_1 = V_c Y_1 = V_c / Z_1 \tag{16}$$

For B-Phase

$$V_B/Z_2 = V_B. Y_2 = I_2 \tag{17}$$

$$I_1 = I_B - I_C + I_2 \tag{18}$$

$$I = I_A - I_B - I_2 \tag{19}$$

In (16) and (17), Y_1 and Y_2 are the effective externally connected admittances across C-phase and B-phase, respectively. Equation (15) implies that zero-sequence voltages and currents are absent in the SEIG. Solving the above equations in association with the symmetrical component equations for a delta-connected system [12], the positive-sequence voltage V_p and negative-sequence voltage V_n can be determined:

$$V_p = \sqrt{3} V [Y_n + Y_1 (e^{-j\pi/6} / \sqrt{3}) + Y_2 (e^{j\pi/6} / \sqrt{3})] / [Y_1 + Y_2 + Y_p + Y_n] \tag{20}$$

$$V_n = \sqrt{3} V [Y_p + Y_1 (e^{j\pi/6} / \sqrt{3}) + Y_2 (e^{-j\pi/6} / \sqrt{3})] / [Y_1 + Y_2 + Y_p + Y_n] \tag{21}$$

The voltage across terminals 1 and 3 in Fig. 2 is given by

$$V = (V_p / \sqrt{3})(h-h^2)[Y_1+Y_2+Y_p+Y_n] / [h Y_2 +(h-h^2) Y_n - Y_1 h^2] \tag{22}$$

Where h is the complex operator $e^{(j 2\pi/3)}$. The input current I is given by ;

$$I = (V_p/\sqrt{3})(h-h^2)[(Y_1+Y_2)(Y_p+Y_n) + (3Y_pY_n+Y_1Y_2)] / [hY_2+(h-h^2)Y_n-Y_1h^2] \tag{23}$$

From (22) and (23), the input impedance Z_{in} of the SEIG when viewed across terminals 1 and 3 is given by

$$Z_{in} = (Y_1 + Y_2 + Y_p + Y_n) / [(Y_1 + Y_2)(Y_p + Y_n) + 3 Y_p Y_n + Y_1 Y_2] \quad (24)$$

Both Y_p and Y_n are functions of the per-unit frequency a and the magnetizing reactance X_m , hence the input impedance of the SEIG may be written as:

$$Z_{in} = R_{in}(a, X_m) + j X_{in}(a, X_m) \quad (25)$$

From (24), the SEIG system of Fig. 2 may be reduced to the circuit has been shown in Fig. 3. Applying KVL to the latter circuit,

$$I(Z_3 + Z_{in}) = 0 \quad (26)$$

Current I can not = 0, hence

$$(Z_3 + Z_{in}) = 0 \quad (27)$$

The complex equation (27) must be solved to determine the X_m . After a and X_m have been determined, the positive-sequence air gap voltage is found from the magnetization curve. The generator performance can then be computed using (14)–(23) together with the symmetrical component equations.

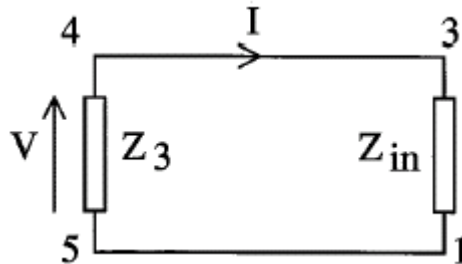


Fig. 3. Simplified circuit of three-phase SEIG.

VI. SOLUTION TECHNIQUE

The input impedance Z_{in} as given by (24) involves the generator admittances Y_p and Y_n whose real and imaginary parts are high-order polynomials of a and X_m . Due to the algebraic manipulations prescribed by (24), both are complicated functions of the above two variables. It is thus extremely difficult to solve (27) using conventional techniques such as the Newton–Raphson method [1] or the polynomial method [13], due to the complicated mathematical derivations required. To reduce the computational efforts, a function minimization technique is employed for solving (27). This is based on the observation that, for given values of X_m and a , the input impedance Z_{in} can be computed readily. It can be shown that the values of X_m and a that satisfy (27) will also result in a minimum value (of zero) in the following scalar impedance function:

$$Z(a, X_m) = [(R_3 + R_{in})^2 + (X_3 + X_{in})^2]^{1/2} \quad (28)$$

where R_3 and X_3 are respectively the equivalent series resistance and reactance of the terminal impedance Z_3 . This method employs two search strategies, namely *exploratory moves* and *pattern moves*, in order to arrive at the optimum point. A function evaluation is required each time an exploratory move or pattern move is to be made. For normal operation of an SEIG, is slightly less than the per-unit speed b while X_m is less than the unsaturated value X_{mu} , hence b and X_{mu} could in general be chosen as initial estimates for a and X_m for starting the search procedure. Over a wide range of load and for various unbalanced cases, convergence can be obtained in 350 to 450 function evaluations for the experimental machine. Subsequent research on the Steinmetz connection for SEIGs reveals that additional circuit elements are required in order to achieve perfect phase balance. Based on this result, a modified Steinmetz connection (MSC) for a three-phase SEIG is proposed in this paper. Fig. 4 shows the circuit connection of the MSC, where all circuit parameters have been referred to the base frequency. The impedance Z_3 across –A phase (the reference phase) consists of the main load resistance R_{L3} and the auxiliary excitation capacitance in parallel. The impedance Z_2 across B-phase (the lagging phase) consists of the main excitation capacitance C_2 and auxiliary load resistance R_{L2} in parallel. Compared with the original Steinmetz connection [22], it is seen that the auxiliary resistance R_{L2} and the auxiliary excitation capacitance C_3 have been introduced. For a practical SEIG system, R_{L2} could be local loads such as lighting, storage heating, or battery charging. Alternatively, R_{L2} could be a portion of the remote loads. The three-phase SEIG with MSC can also be analyzed using the general method described in Sections V and VI. In this case, R_{L2} is equal to zero while Y_2 and Y_3 are the resultant admittances connected across phase A and B phase , respectively.

A. Conditions for Perfect Phase Balance

Figure 5 shows the phasor diagram of the three-phase SEIG with MSC under balanced conditions, it being assumed that the positive- sequence impedance angle Φ_p is greater than $2\pi/3$ radian. The line current I_{L2} flowing into terminal 2 consists of the current through the main excitation capacitance C_2 and the current I_{R2} through the auxiliary resistance. Meanwhile, the line current I_{L3} flowing into terminal 3 is contributed by $-I_{R3}$ (where I_{R3} is the main load current) as well as $-I_{C3}$ (where I_{C3} is the current through the auxiliary capacitance C_3). The current components I_{R2} and I_{C3} enable balanced line currents of the SEIG to be synthesized. A careful study of the relationship between the current and voltage phases in Fig. 5 presents the under perfect phase balance, the angle between and is equal to radian. while the angle γ between I_{C2} and I_{L2} is equal to $(\Phi_p - 2\pi/3)$ radian. while the angle δ between $-I_{R3}$ and I_{L3} is equal to $(5\pi/6 - \Phi_p)$ rad. Since each current in the phasor triangles opq and omn may be expressed in terms of the phase voltage and the associated admittance, conductance or susceptance, the following relationships can be derived;

$$G_2 = \sqrt{3} | Y_p | \sin (\Phi_p - 2\pi / 3) \quad (29)$$

$$B_2 = \sqrt{3} | Y_p | \cos (\Phi_p - 2\pi / 3) \quad (30)$$

$$G_3 = \sqrt{3} | Y_p | \cos (5 \pi / 6 \Phi_p - \Phi_p) \quad (31)$$

$$B_3 = \sqrt{3} | Y_p | \sin (5 \pi / 6 \Phi_p - \Phi_p) \quad (32)$$

Where $G_2 = a / R_{L2}$; $B_2 = a^2 2\pi f_{base} C_2$; $G_3 = a / R_{L3}$ and $B_3 = a^2 2\pi f_{base} C_3$.

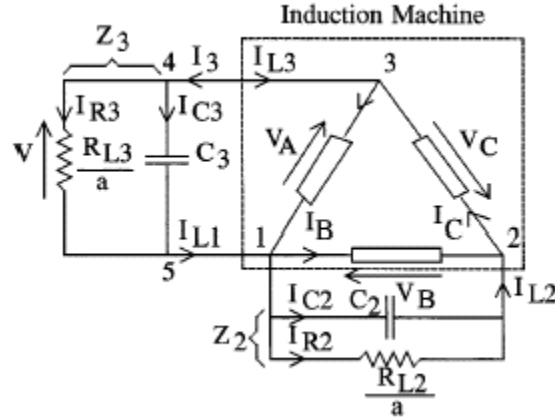


Fig. 4. Modified Steinmetz connection (MSC) for three-phase SEIG.

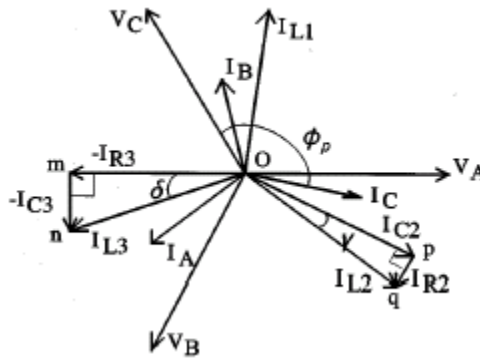


Fig. 5. Phasor diagram for SEIG with MSC under perfect phase balance δ

When Φ_p is greater than $2\pi/3$ radian (which corresponds to a heavy load condition), G_2 is positive and perfect balance can be obtained with all four circuit elements in Fig. 4 present. When Φ_p is equal to $2\pi/3$ radian, G_2 vanishes showing that phase balance can be achieved with the auxiliary load resistance removed. Under this condition, $G_2 = 0$, and $\sqrt{3} Y_p = B_2$, $(1/2)\sqrt{3} Y_p = B_3$, $(1/2)3 Y_p = G_3$. When Φ_p is less than $2\pi/3$ radian, however, G_2 is negative and perfect phase balance cannot be obtained with passive circuit elements. Equation (32) shows that B_3 vanishes when $\Phi_p = 5\pi/6$ radian, which implies that the auxiliary capacitance C_3 can be dispensed with. When Φ_p exceeds $5\pi/6$ radian, B_3 becomes negative, implying that perfect balance can be achieved with an auxiliary inductance across A-phase. In practice, however, the full-load power factor angle of an SEIG ranges from $2\pi/3$ radian to $4\pi/3$ radian, hence it is very unlikely that an inductive element need to be used.

VII. SELECTION OF LOAD AND PHASE CONVERTER

A practical design problem is, for a given speed and main load Resistance R_{L3} , from (29) – (32), it is observed that G_2 , B_2 , G_3 and B_3 are all functions of the variables Y_p and Φ_p which depend on the terminal impedances. An iterative procedure is therefore required to give perfect phase balance. For convenience, Φ_p can first be specified while Y_p is to be determined during the iterations. The iterative procedure may be summarized as follows:

- 1) Input the per-unit speed and specified value of Φ_p .
- 2) Assume an initial value of the per-unit frequency 'a'.
- 3) For a given value of main load resistance R_{L3} , compute $|Y_p|$ from (29) using the current value of a.
- 4) Compute B_2 , G_3 , B_3 and using (30) – (32).
- 5) Compute Y_2 and Y_3 (hence R_3 and X_3) in Fig. 2, using the values of circuit elements obtained in steps (3 and 4).
- 6) Determine a and X_m using the Hooke and Jeeves method outlined in the section VI.
- 7) Repeat steps (3 – 6) until the values of in successive iterations is less than a specified value.
- 8) Compute the values of phase converter elements and performance of the SEIG using the final values of a and X_m .

VIII. CONCLUSION

The pattern search method presented by Hooke and Jeeves has been applied for the determination of the per unit frequency and magnetizing reactance. Due to the phase-balancing action of the excitation capacitance and the load compensation effect of the series capacitance, very good phase balance is obtained over a wide range of load current. With an appropriate choice of shunt and series value of the excitation capacitances. Balanced three-phase operation is achieved at a certain load, giving good winding utilization, a large power output, high efficiency, and a small voltage regulation.

REFERENCES

- [1] A. H. Al-Bahrani and N. H. Malik, "Steady state analysis and performance characteristics of a three phase induction generator self-excited with a single capacitor," *IEEE Trans. Energy Conversion*, vol. 5, no. 4, pp. 725–732, Dec. 1990.
- [2] A. I. Alolah and M. A. Alkanhal, "Excitation requirements of three phase self excited induction generator under single phase loading with minimum unbalance," in *Proceedings of IEEE Power Engineering Society 2000 Winter Meeting*, Singapore, Jan. 23–27, 2000.

- [3] B. Singh, R. B. Saxena, S. S. Murthy, and B. P. Singh, "A single-phase self-excited induction generator for lighting loads in remote areas," *International Journal on Elect. Engg. Education*, vol. 25, pp. 269–275, 1988.
- [4] B. S. Gottfried and J. Weisman, *Introduction to Optimization Theory*. Englewood Cliffs, NJ: Prentice Hall Inc., 1973.
- [5] C. Chakraborty, S. N. Bhadra, and A. K. Chattopadhyay, "Analysis of parallel-operated self-excited induction generators," *IEEE Trans. Energy Conversion*, vol. 14, no. 2, pp. 209–216, June 1999.
- [6] D. B. Watson, J. Arrillaga, and T. Densem, "Controllable d.c. power supply from wind driven self-excited induction machines," *Proceedings of IEE*, vol. 126, no. 12, pp. 1245–1248, 1979.
- [7] E. Bim, J. Szajner, and Y. Burian, "Voltage compensation of an induction generator with long-shunt connection," *IEEE Trans. Energy Conversion*, vol. EC-4, no. 3, pp. 526–530, Sept. 1989.
- [8] E. Profumo, B. Colombo, and F. Mocci, "A frequency controller for induction generator in standby minihydro power plants," in *4th International Conference on Electrical Machines and Drives*, 1989, IEE Publication no. 310, pp. 256–260.
- [9] G. Raina and O. P. Malik, "Wind energy conversion using a self-excited induction generator," *IEEE Trans. Power Apparatus and Systems*, vol. PAS-102, no. 12, pp. 3933–3936, Dec. 1983.
- [10] J. E. Brown and C. S. Jha, "The starting of a 3-phase induction motor connected to a single-phase supply system," *Proc. of IEE*, vol. 106A, pp. 183–190, 1959.
- [11] J. E. Brown and O. I. Butler, "A general method of analysis of 3-phase induction motors with asymmetrical primary connections," *Proc. of IEE*, pt. II, vol. 100A, pp. 25–34, 1953.
- [12] J. E. Brown and C. S. Jha, "The starting of a 3-phase induction motor connected to a single-phase supply system," *Proc. of IEE*, vol. 106A, pp. 183–190, 1959.
- [13] L. Ouazene and G. McPherson, Jr., "Analysis of the isolated induction generator," *IEEE Trans. P.A.S.*, vol. PAS-102, no. 8, pp. 2793–2798.
- [14] M. G. Say, *Alternating Current Machines*, 5th ed. London: Pitman (ELBS), 1983, pp. 333–336.
- [15] R. Holland, "Appropriate technology—Rural electrification in developing countries," *IEE Review*, vol. 35, no. 7, pp. 251–254, 1989.
- [16] S. S. Murthy, O. P. Malik, and A. K. Tandon, "Analysis of self-excited induction generators," *Proceedings of IEE*, pt. C, vol. 129, no. 6, pp. 260–265, Nov. 1982.
- [17] S. S. Murthy, "A novel self-excited self-regulated single phase induction generator Part 1: Basic system and theory," *IEEE Trans. Energy Conversion*, vol. 8, no. 3, pp. 377–382, Sept. 1993.
- [18] T. Fukami, Y. Kaburaki, S. Kawahara, and T. Miyamoto, "Performance analysis of a self-regulated self-excited single-phase induction generator using a three-phase machine," in *1997 IEEE International Electric Machines and Drives Conference Record*, Milwaukee, WI, USA, May 18–21, 1997, pp. TD2-3.1–TD2-3.3.

- [19] T. F. Chan, "Performance analysis of a three-phase induction generator connected to a single-phase power system," *IEEE Trans. Energy Conversion*, vol. 13, no. 3, pp. 205–211, Sept. 1998.
- [20] T. F. Chan, "Performance analysis of a three-phase induction generator self-excited with a single capacitance," in *IEEE Transactions on Energy Conversion*, Paper no. PE-028-EC-0-10-1997.
- [21] Y. H. A. Rahim, A. I. Alolah, and R. I. Al-Mudaiheem, "Performance of single phase induction generators," *IEEE Trans. Energy Conversion*, vol. 8, no. 3, pp. 389–395, Sept. 1993.
- [22] ---, "Performance analysis of a three-phase induction generator self-excited with a single capacitance," in *IEEE Power Engineering Society 1998 Winter Meeting*, Tampa, FL, USA, Feb. 1–5, 1998,

APPENDIX

The positive-sequence impedance Z_p and negative-sequence impedance Z_n of the induction machine are given as follows:

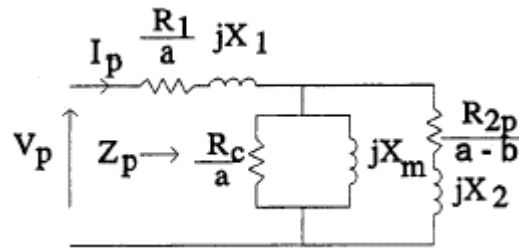


Fig. 6. Positive-sequence impedance Z_p of induction machine.

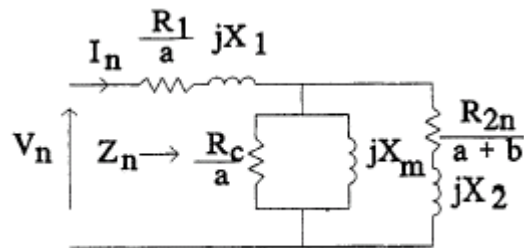


Fig. 7. Negative-sequence impedance Z_n of induction machine.